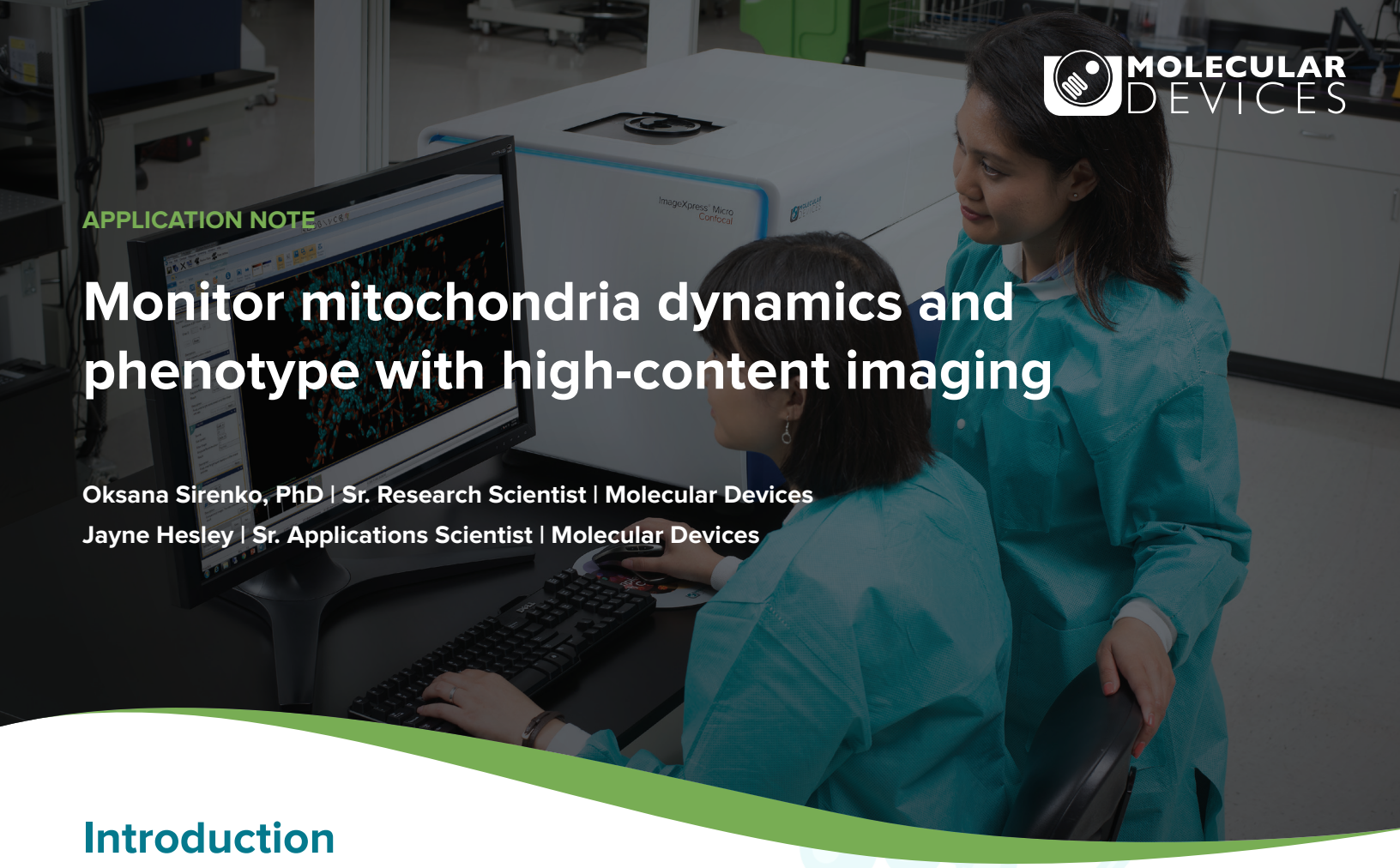

APPLICATION NOTE

Monitor mitochondria dynamics and phenotype with high-content imaging

Oksana Sirenko, PhD | Sr. Research Scientist | Molecular Devices

Jayne Hesley | Sr. Applications Scientist | Molecular Devices

Introduction

Mitochondria are the main energy source for cells and play a key role in regulating cellular metabolism. Mitochondria can change their structures depending on environmental conditions and cellular requirements. The dynamic nature of mitochondria is driven by several processes that regulate mitochondrial morphology including fission, fusion, mitophagy, and biogenesis.

Fission creates larger amounts of mitochondria that are circular in shape and smaller in size. Fusion creates smaller amounts of mitochondria that are elongated in shape and larger in size. The opposing processes of mitochondrial fission and fusion are both involved in mitochondrial quality control and the maintenance of normal cellular homeostasis[2, 3]. Both fission and fusion are critical to normal cellular function.

Mitophagy is a process for clearing damaged mitochondria, and a critical component of normal mitochondrial recycling[3]. A damaged or senescent mitochondrion undergoes asymmetric fission. While the healthy components are delivered to the new mitochondria, the damaged components are segregated into the smaller components that are depolarized and promptly eliminated via mitophagy[4]. Biogenesis is the process that results in synthesis of new mitochondrial components.

Pathologic alterations in mitochondrial dynamics can result in impaired bioenergetics and mitochondrial-mediated cell death, and are associated with a wide spectrum of pathologies, including ischemic cardiomyopathy, diabetes, pulmonary hypertension, Parkinson's and Huntington's diseases and skeletal muscle atrophy, or Alzheimer's disease[1, 5]. Neurons are particularly sensitive to changes in mitochondrial function due to their limited capacity for glycolysis and high level of energetic use[6]. Cardiomyocytes, which have one of the highest volume fractions of mitochondria are also uniquely sensitive to mitochondrial dynamic alterations[7, 8]. Mitochondrial dynamic alterations also play a role in many cancers, where fusion can reduce the susceptibility of cells to apoptotic signaling, induce aerobic glycolysis (the Warburg effect), and potentially enhance cancer cell growth by reducing apoptotic cell death[9].

Benefits

- Acquire high-quality images and achieve better visualization of changes in mitochondrial shape and structure
- Quantify and measure phenotypic changes in mitochondria in a more efficient and precise manner
- Understand mechanisms of disease and assess compound toxicity in a variety of cell models

Alterations in mitochondrial dynamics can be a normal physiologic response to stress. Studies in skeletal muscle during exercise suggest a role for mitochondrial fragmentation in maintaining energetic homeostasis. During recovery, fusion is activated, and with chronic exercise, mitochondrial biogenesis[10].

There has been growing interest in using high-content imaging methods for studying the mitochondrial structure remodeling. Confocal imaging and water immersion objectives can offer enhanced image quality and better visualization of mitochondria structures, while the tools of image analysis can be utilized to obtain numeric characterization of different phenotypes. In this study, we describe phenotypic assays for mitochondria phenotypes and structural re-arrangements that can be used for studies of mitochondria dynamics in cell-based assays.

Materials

Human neuroblastoma PC12 cells were obtained from ATCC. Hoechst 33342 and MitoTracker Orange CMTMRos were purchased from Thermo Fisher. Chemical compounds were purchased from Sigma.

Method

Human neuroblastoma PC12 cells were plated in Greiner 384-well plates at a density of 3,000 cells per well. The next day, cells were treated for 18 hours with various concentrations of several benchmark compounds known to effect mitochondria: chloroquine (0 – 100 µM), rotenone (0 – 10 µM), valinomycin (0 – 1 µM), and methyl mercury (0 – 10 µM). Each compound was tested at seven different concentrations, half-log dilutions, in quadruplicates for a sample size of n = 8. After treatment, live cells were stained with a combination of mitochondrial dye Mitotracker Orange CMTMRos and Hoechst 33342 nuclear dye (0.2 µM and 0.5 µM, respectively) for 30 min, and imaged with the ImageXpress® Micro Confocal system (Molecular Devices). Images of live cells were taken using confocal mode and the 40X water immersion objective. Three to four sites were imaged for each well. For better assay performance, a z-stack of 3–4 image planes was acquired at 0.6–1 µm intervals. Nuclei were imaged with the DAPI channel and mitochondria with the TRITC channel, at 100 ms and 400 ms exposures respectively. Images were analyzed using the Custom Module Editor in MetaXpress® High-Content Image Acquisition and Analysis Software. Details are described in more detail in the Results section. Briefly, a Find Fibers module was used to identify elongated mitochondria, and the Granularity module for more round particles. Cell boundaries were outlined for counting objects per cell. Secondary analysis was completed using Excel or SoftMax® Pro Software curve fitting tools. Z' values were calculated using the formula Z' = 1-3*(STDEVcontrol+ STDEVexperiment)/(AVEcontrol-AVEexperiment).

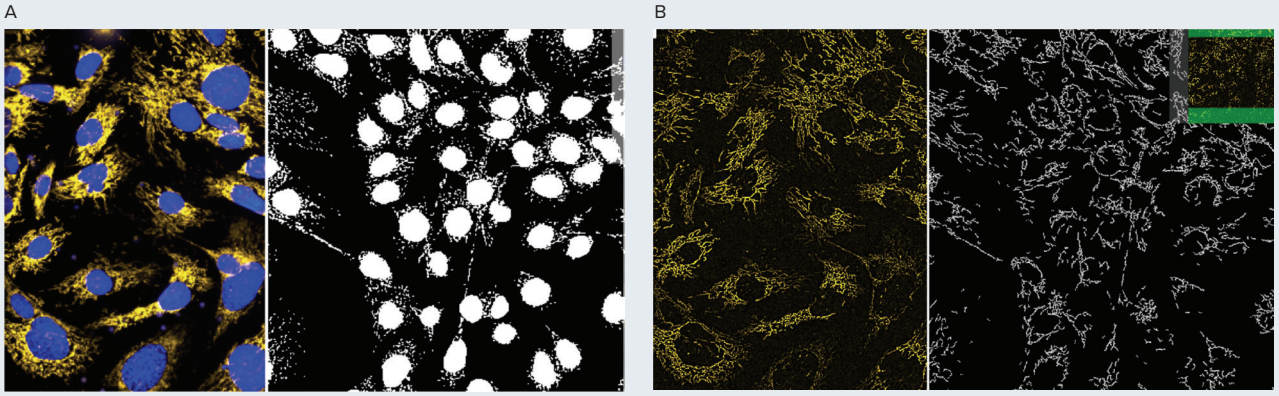

Figure 1. *Phenotypic analysis of mitochondria shape. PC12 neuroblastoma cells were stained with MitoTracker Orange and Hoechst for 15 min and imaged with IXM-C using the 40X water immersion objective in confocal mode. Images were analyzed using Granularity (A) and Find Fibers (B) modules of MetaXpress Custom Module Editor. A. Nuclei are shown in blue and intact mitochondria in yellow. The split image shows masks for nuclei and mitochondria (granules) in white on the right. B. Mitochondria images in yellow were pre-processed with an image sharpening algorithm (Top Hat). The split image on the right shows masks of the 'fiber' structures.*

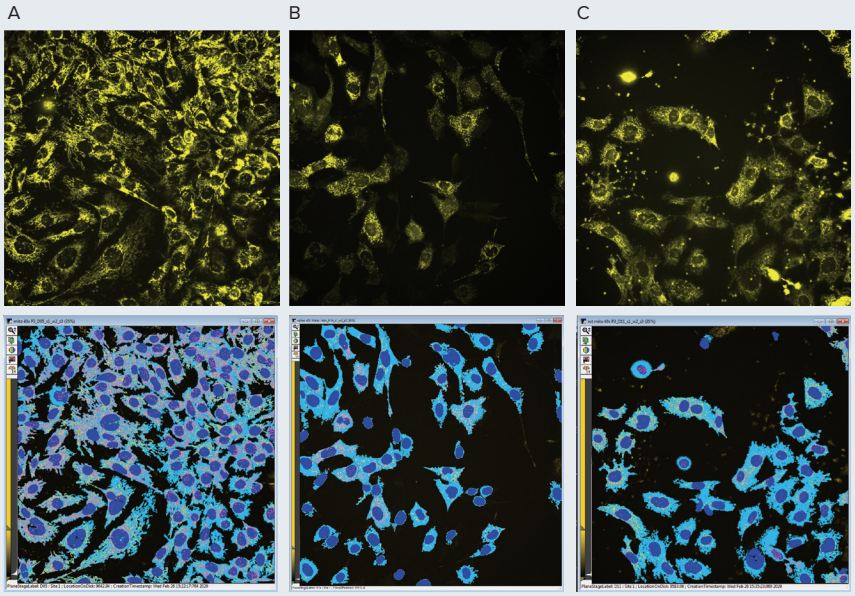

Figure 2. *Compounds effect on mitochondria. Top panel shows MitoTracker CMTMRos mitochondria stain (yellow) for control PC12 neuroblastoma cells (A), or cells treated for 18 hours with 100 nM of compounds known to cause damage to mitochondria: valinomycin (B) and rotenone (C). Cells were imaged with the IXM-C using the 40X water immersion objective with confocal mode. The brightness display of images was adjusted to allow better visualization of mitochondria. Note the changes in mitochondria shape: fragmentation of mitochondria threads to smaller particles with valinomycin, and tangling and collapsing mitochondria with rotenone. Images were analyzed using MetaXpress Custom Module Editor. Analysis masks in the bottom panel show mitochondria granules (pink) and fiber structures (yellow), nuclei (dark blue), and cell bodies (light blue).*

Results

Characterizing mitochondria integrity and shape is important for understanding mechanisms of disease and assessing toxicity. The number, brightness, size, length and shape of mitochondria change during mitochondria recycling and may indicate cell health and metabolic changes, or precede the process of apoptosis. We have compared phenotypes of mitochondria of control PC12 neuroblastoma cells with changes caused by compounds known to affect mitochondria: chloroquine, which inhibits mitochondria recycling, rotenone, an inhibitor of oxidative phosphorylation, and valinomycin, potassium ionophore, which disrupts mitochondria membrane potential. Cells were treated with various concentrations of compounds, in quadruplicates, for 18 hours. Images of cells stained with MitoTracker Orange and Hoechst nuclear dye taken in confocal mode with the 40X water immersion objective allowed ability to resolve individual mitochondria and monitor changes in mitochondria shapes.

Figures 1 and 2 show images of mitochondria, control samples and samples treated with compounds. For example, note the changes in the mitochondria phenotypes presented in Figure 2. Control cells show long stretches of mitochondria fibers, while treatment with valinomycin resulted in mitochondria fragmentation and fission, as observed by the appearance of mitochondria as smaller dots. Treatment with rotenone caused mitochondria fragmentation and condensation around the nuclei. Importantly, both valinomycin and rotenone caused loss of mitochondria potential reflected in decreased fluorescent intensities for mitochondria (Figure 2). The effect of chloroquine was not obvious by visual observation, but apparent changes in morphology were evident as a result of image analysis measurements (see below). We observed concentration-dependence of compound effects (Figure 2). Morphological changes were clearly observed with lower concentrations of compounds. Higher concentrations of compounds caused loss of mitochondria potential, disruption of mitochondria, and progressive cell death.

 |

Morphometric measurements were derived by using tools of MetaXpress software. We utilized Custom Module Editor to allow finding and characterization of objects that can be defined as “granules” or as “fibers”. Granules were defined by the Granularity module; fibrous structures, or segments, can be determined by the Find Fibers module. Structures are determined by user-defined criteria, like minimum and maximum width, and intensity over local background. Image pre-processing (sharpening) was used as an optional step for better definition of fibers (Figure 1). The numbers of objects, areas, intensities, lengths, and shape can be defined for each object and presented as averages or sums of values, on a per cell, or per image basis (Figure 2). These measurements can describe the numbers and phenotypes to characterize mitochondria structural dynamics (Figure 4), as well as calculate dose-responses and effective concentrations of various compounds (Figure 3). Specifically, treatment with agents that are known to be toxic for mitochondria not only resulted in decreased mitochondria potential (detected as decreased numbers and intensities for mitochondria particles, both granules and fibers), but also changes in the total and average fiber length, especially notable for treatment with valinomycin (Figure 4). In contrast, treatment with chloroquine, which inhibits mitochondria recycling, resulted in accumulation of mitochondria, and therefore an increase in the number of fibers.

Table 2 presents comparisons of different measurements for control and compound treated samples. Data are presented for single (intermediate) concentrations of compounds: 20 µM chloroquine, 300 nM rotenone, and 100 nM valinomycin. Marked dose-dependent decrease in the number and length of mitochondria fibers was observed after treatments with rotenone and valinomycin, while chloroquine caused an opposite effect. The numbers and areas of granules determined by Granularity analysis was also decreased with valinomycin and rotenone. This method allows one to derive various measurements, and this multi-parametric approach can be used for defining effects of signaling pathways or compound effects on multiple aspects of complex biological changes.

During assay development, we compared the impact of water immersion objectives to air objectives on image quality and analysis. Notably, using water immersion objectives improved quality of images and typically resulted in increased Z’ values (Table 3). The present analysis is not exclusive between fibers and granules, so values for fibers and granules were counted independently using the recommended protocol. The description of the Custom Module used is presented in the Figure 5. It can be adjusted and further modified for specific cell type or disease model.

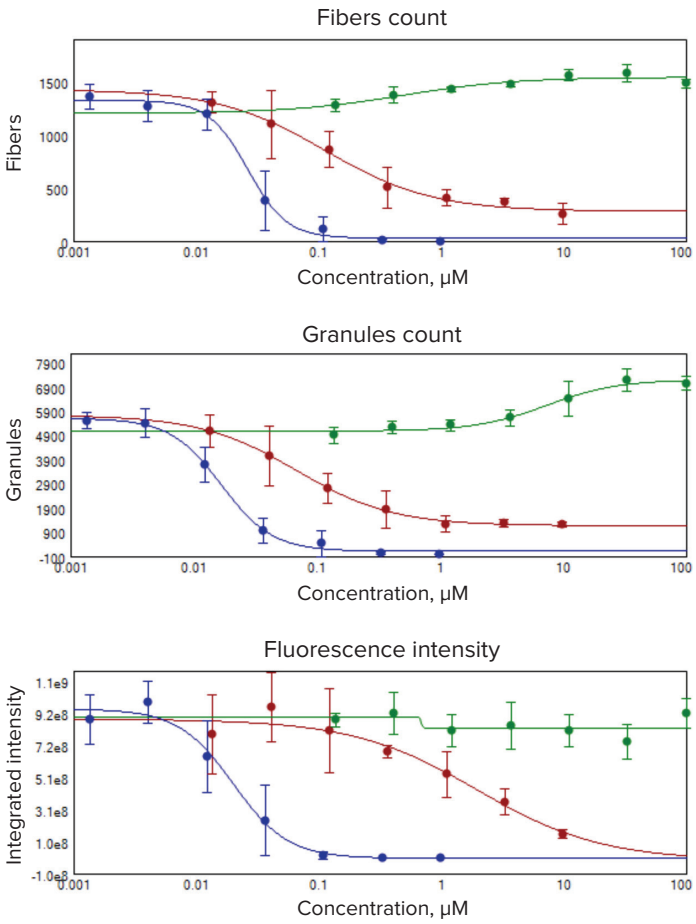

Figure 3. *Concentration-dependencies of PC12 neuroblastoma cells were treated with chloroquine, which inhibits mitochondria recycling, rotenone, an inhibitor of oxidative phosphorylation, and valinomycin, potassium ionophore, which disrupts mitochondria membrane potential. Cells were treated with indicated concentrations of compounds in quadruplicates for 18 hours. Cells were stained and imaged as described in Figures 1 and 2. Image analysis identified mitochondria structures as “fibers” (top) or “granules” (middle). EC_{50} values were calculated from concentration-dependencies using quadruplicate samples and 4-parametric curve fit. Additional plot represents changes in the fluorescence intensity for mitochondria stain. Chloroquine is shown in green, rotenone in red, and valinomycin in blue.*

EC_{50}, nM	Fibers Count	Granules Count
Rotenone	112 ± 30	68 ± 10
Chloroquine	488 ± 1000	7260 ±2000
Valinomycin	26 ± 2.3	17 ± 2.0

Table 1. *EC_{50} values were quantitated from the curves shown in Figure 3.*

 |

	Control	Rotenone	Chloroquine	Valinomycin
Cell count	44.5 ± 9.5	30 ± 5.5	46 ± 8.7	57 ± 11
Fiber count (total)	2606 ± 250	564 ± 47	3791 ± 287	32 ± 44
Fiber Length Ave (µm)	4.4 ± 0	3.9 ± 0.1	5.3 ± 0.3	2.7 ± 0.2
Fibers (per cell)	131 ± 34.7	8 ± 1	383 ± 57.4	1 ± 0.9
Fiber Length Sum (per cell)	431 ± 87.3	68 ± 15.3	3457 ± 912	54 ± 11
Granules (total)	4739 ± 413	963 ± 131	8088 ± 887	105 ± 54
Granules (per cell)	97 ± 24.8	5 ± 1.3	529 ± 94	2 ± 1.2
Granule Area Sum (per cell)	114 ± 39.6	18 ± 0.7	609 ± 231	0
Granule Ave Intensity	1009 ± 47.8	1342 ± 73.1	1068 ± 43.1	944 ± 23.1

Table 2. *Comparison of different measurements for control and compound treated samples. Data presented are for control sample, 10 µM of chloroquine, 300 nM of rotenone, and 10 nM of valinomycin*

Z' value	WI 40X	Air 40X
Total Fibers	0.52	0.42
Total Granules	0.55	0.41
Total Segments	0.5	0.38

Table 3. *Water immersion objectives improved quality of images and resulted in more accurate identification of the numbers of particles with resulting higher Z-values compared to air objectives.*

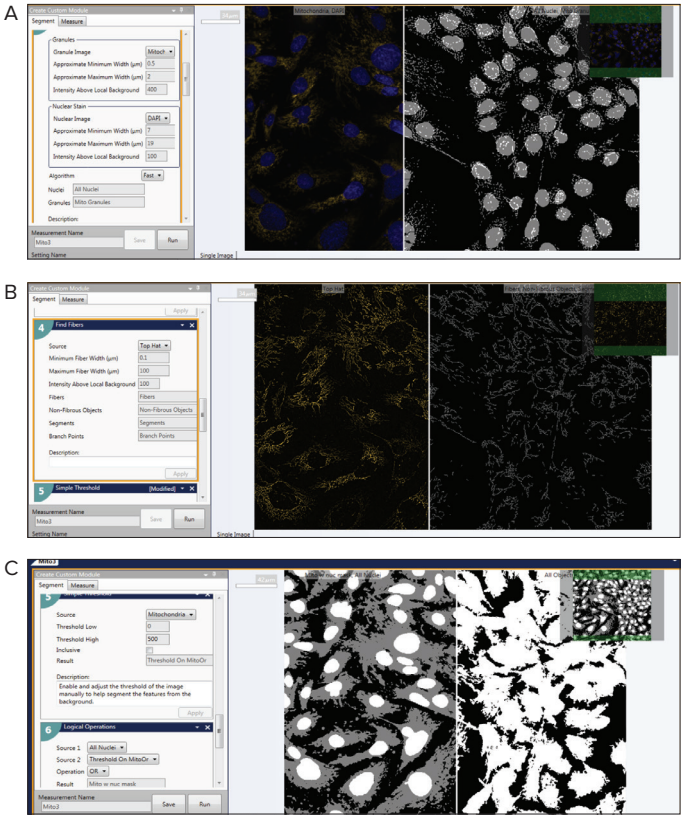

Figure 4. *Custom Module Editor (description). Custom Module Editor was designed to count and analyze the phenotypes of mitochondria for assessment of mitochondria health, metabolism, recycling, compound effects and implication of the status of diseases.*

The module includes the following steps:

1. *Granularity module, to detect mitochondria particles.*
2. *Pre-processing of mitochondria image with Top Hat filter.*
3. *Find Fibers module to detect mitochondria particles and their fission and fusion.*
4. *Simple Threshold to identify cell bodies.*

The measurements for each object can be applied to determine total numbers of objects in each image, or per each cell, as defined by the final step in the custom module. The relevant measurements depend on the specific application. We found the most interesting measurements as:

1. *Nuclei count (cell count)*
2. *Nuclear average area/average intensity*
3. *Total Granules (per site)*
4. *Cells: Granules (per cell)*
5. *Granule Area Ave, Granule Area Sum, Granule Intensity Ave or Integrated Intensity Ave*
6. *Total Fibers (per image)*
7. *Cells: Fibers (per cell)*
8. *Fibers Length Ave, Fibers Length Sum, Fibers Intensity Ave*

Conclusion

We described here the method for analysis of mitochondria dynamics using high-content imaging and advanced image analysis. The proposed method enables quantification of phenotypic changes in mitochondria, and can be used for studies of normal and pathological structural changes to characterize disease phenotypes or compound effects. Automated imaging can be applicable for drug development or toxicity assessment of compounds in various cell models.

References

1. Roberta A. Gottlieb, M.D., and Daniel Bernstein, M.D. Mitochondrial Remodeling: Rearranging, Recycling, and Reprogramming. Cell Calcium. 2016 Aug; 60(2): 88–101.
2. Yisang Yoon, Eugene W Krueger, Barbara J Oswald, Mark A McNiven. The Mitochondrial Protein hFis1 Regulates Mitochondrial Fission in Mammalian Cells Through an Interaction With the Dynamin-Like Protein DLP1. Mol Cell Biol , 23 (15), 5409-20 2003
3. McLelland GL, Soubannier V, Chen CX, McBride HM, Fon EA. Parkin and PINK1 function in a vesicular trafficking pathway regulating mitochondrial quality control. EMBO J. 2014;33:282–295.
4. Twig G, Elorza A, Molina AJ, Mohamed H, Wikstrom JD, Walzer G, Stiles L, Haigh SE, Katz S, Las G, et al. Fission and selective fusion govern mitochondrial segregation and elimination by autophagy. EMBO J. 2008;27:433–446.
5. Archer SL. Mitochondrial dynamics--mitochondrial fission and fusion in human diseases. N Engl J Med. 2013;369:2236–2251.
6. Qi X, Disatnik MH, Shen N, Sobel RA, Mochly-Rosen D. Aberrant mitochondrial fission in neurons induced by protein kinase C{delta} under oxidative stress conditions in vivo. Molecular biology of the cell. 2011;22:256–265.
7. Yu T, Sheu SS, Robotham JL, Yoon Y. Mitochondrial fission mediates high glucose-induced cell death through elevated production of reactive oxygen species. Cardiovasc Res. 2008;79:341–351.
8. Sang-Bing Ong , Sapna Subrayan, Shiang Y Lim, Derek M Yellon, Sean M Davidson, Derek J Hausenloy. Inhibiting Mitochondrial Fission Protects the Heart Against Ischemia/Reperfusion Injury. Circulation , 121 (18), 2012-22 2010
9. Suen DF, Norris KL, Youle RJ. Mitochondrial dynamics and apoptosis. Genes Dev. 2008;22:1577–1590.
10. Konopka AR, Suer MK, Wolff CA, Harber MP. Markers of Human Skeletal Muscle Mitochondrial Biogenesis and Quality Control: Effects of Age and Aerobic Exercise Training. The journals of gerontology. Series A, Biological sciences and medical sciences 2013.

Contact Us

Phone: +1.800.635.5577
Web: www.moleculardevices.com
Email: info@moldev.com
Check our website for a current listing of worldwide distributors.

Regional Offices

USA and Canada	+1.800.635.5577	China (Beijing)	+86.10.6410.8669	Japan	+81.120.993.656
United Kingdom	+44.118.944.8000	China (Shanghai)	+86.21.3372.1088	South Korea	+82.2.3471.9531
Europe*	00800.665.32860	Hong Kong	+852.3971.3530		

**Austria, Belgium, Denmark, Finland, France, Germany, Ireland, Netherlands, Spain, Sweden and Switzerland*

5/20 2315A
Printed in USA